Supporting Information:

Highly Stable Ordered Intermetallic PtCo Alloy Catalyst Supported on Graphitized Carbon Containing Co@CN for Oxygen Reduction Reaction

Won Suk Jung [a], Woong Hee Lee [b], Hyung-Suk Oh [b, c, d]*, and Branko N. Popov [e]**

[a] Department of Chemical Engineering, Hankyong National University, Jungang-ro 327, Anseong-si, Gyeonggi-do, 17579, Republic of Korea

[b] Clean Energy Research Center, Korea Institute of Science and Technology (KIST), Hwarang-ro 14-gil 5, Seongbuk-gu, Seoul, 02792, Republic of Korea

[c] Division of Energy and Environmental Technology, KIST school, Korea University of Science and Technology, Seoul 02792, Republic of Korea.

[d] KHU-KIST Department of Conversing Science and Technology, Kyung Hee University, Seoul 02447, Republic of Korea.

[e] Center for Electrochemical Engineering, Department of Chemical Engineering, University of South Carolina, Columbia, SC, 29208, USA

* Corresponding author: jungw@khnu.ac.kr, hyung-suk.oh@kist.re.kr, popov@cec.sc.edu

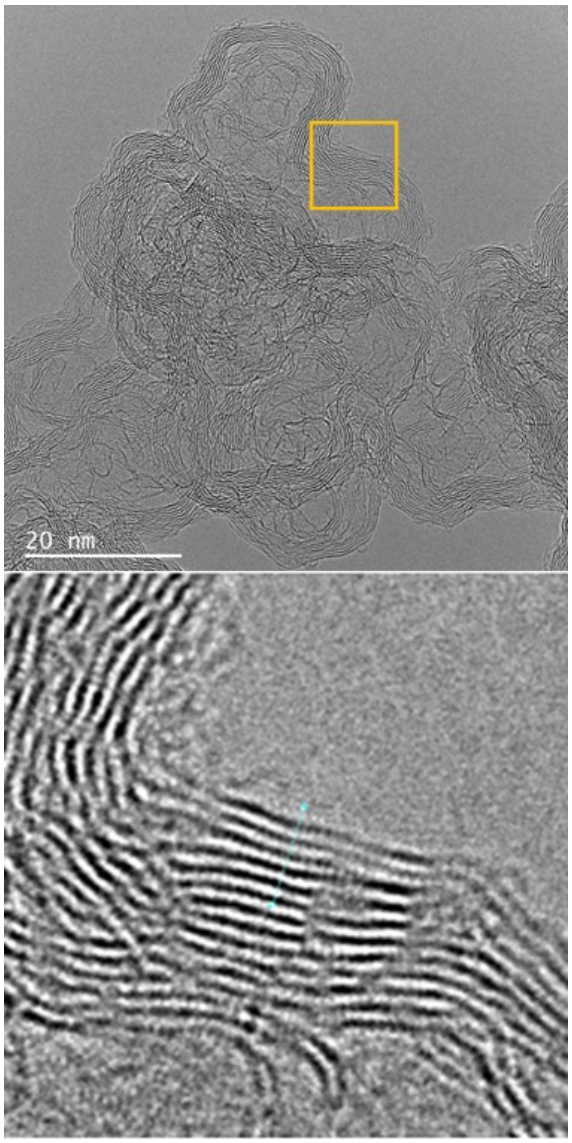

Figure S1. HR-TEM image of GC prepared at 1700 ℃ for 2 h under N_2 atmosphere.

Table S1. Characteristics of Co@CN/GC obtained from XPS N1s peak.

	BE [eV]	FWHM	at. %
Pyridinic- N	398.55	1.374	27.8
Pyrrolic-N and/or pyridone-N	400.18	2.389	37.0
Quaternary-N	401.12	3.026	19.3
Pyridinic-N^{+}-O^{-}	403.70	4.991	15.9

Table S2. Characteristics of Co@CN/GC and CB obtained from XPS C1s peak.

	Co@CN/GC			CB		
	BE [eV]	FWHM	at. %	BE [eV]	FWHM	at. %
graphitic	284.59	0.803	67.7	284.29	0.892	64.4
defect	285.36	0.811	9.8	285.09	1.599	20.4
amine	286.02	1.014	4.0	-	-	-
alcohol and ether	286.54	1.793	8.2	286.57	1.377	4.0
carbonyl	288.01	1.317	2.4	287.98	2.293	4.3
carboxyl	289.11	1.314	1.9	289.09	2.861	1.1
carbonate	290.37	1.448	2.4	290.29	2.075	4.6
π-π* shake-up satellite	291.52	1.874	3.6	291.58	1.47	1.1

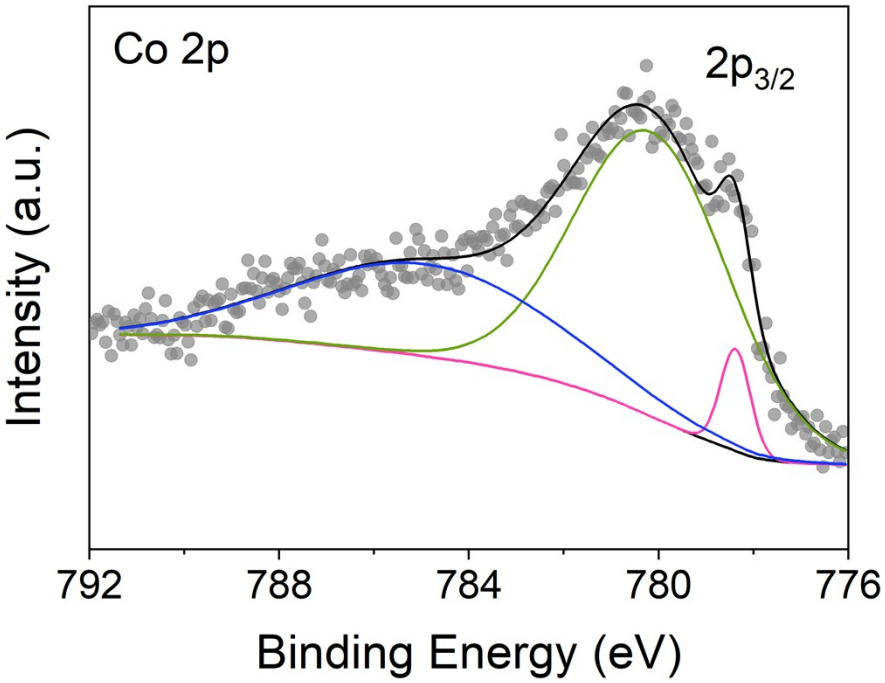

Figure S2. Co 2p XPS spectra of PtCo/NGC

Table S3. Characteristics of PtCo/NGC obtained from XPS Co 2p peak.

	PtCo/NGC		
	BE [eV]	FWHM	at. %
Co^0	778.38	0.734	4.2
Co(II)	780.14	3.843	62.0
Satellites	784.90	6.611	33.9

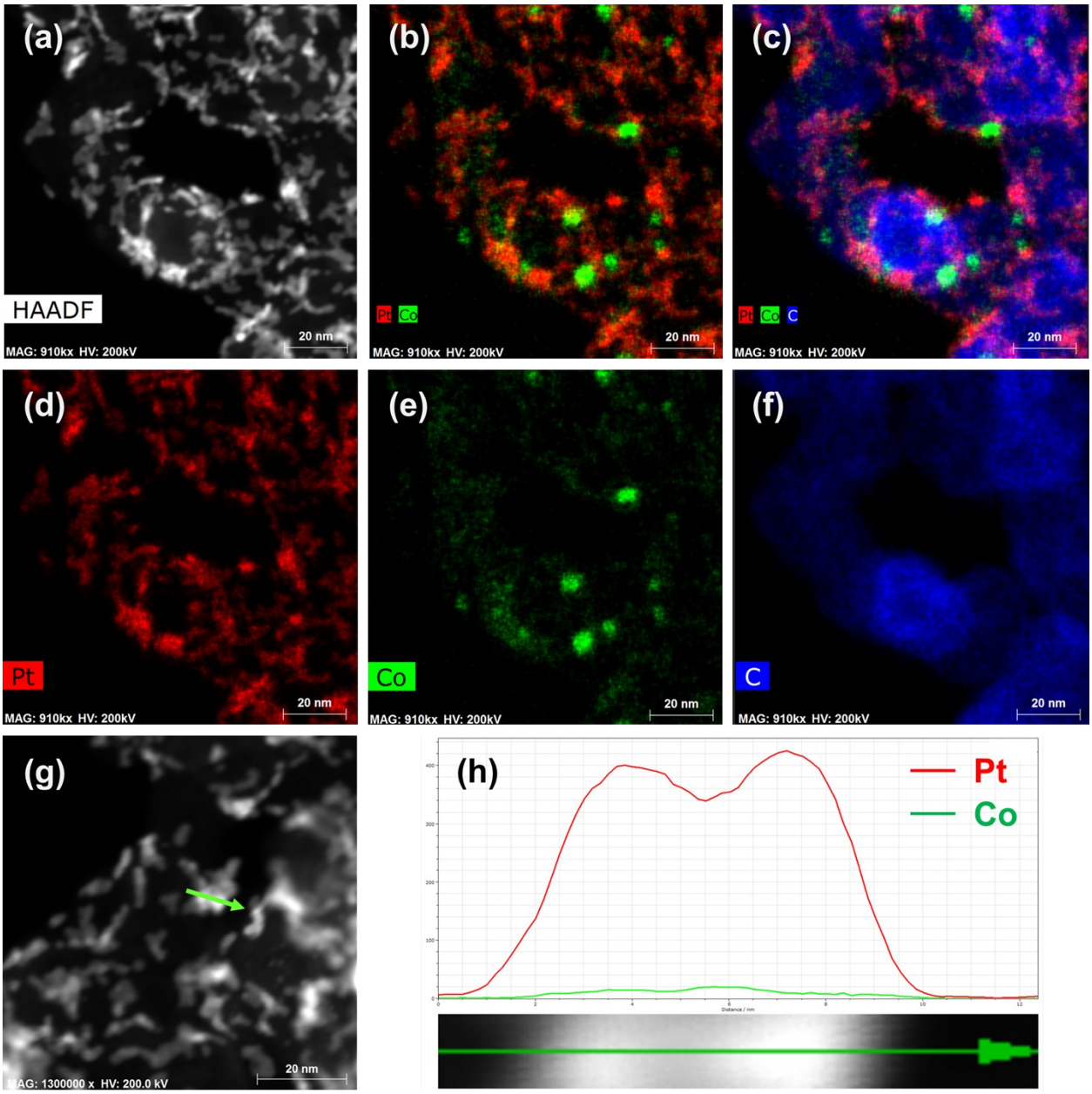

Figure S3. (a) HAADF-STEM image of Pt/Co@CN/GC. EDS elemental mapping images of Pt/Co@CN/GC: (b, c) overlap, (d) Pt, (e) Co, and (f) carbon. (g, h) EDS cross-sectional compositional line profile of Pt/Co@CN/GC.

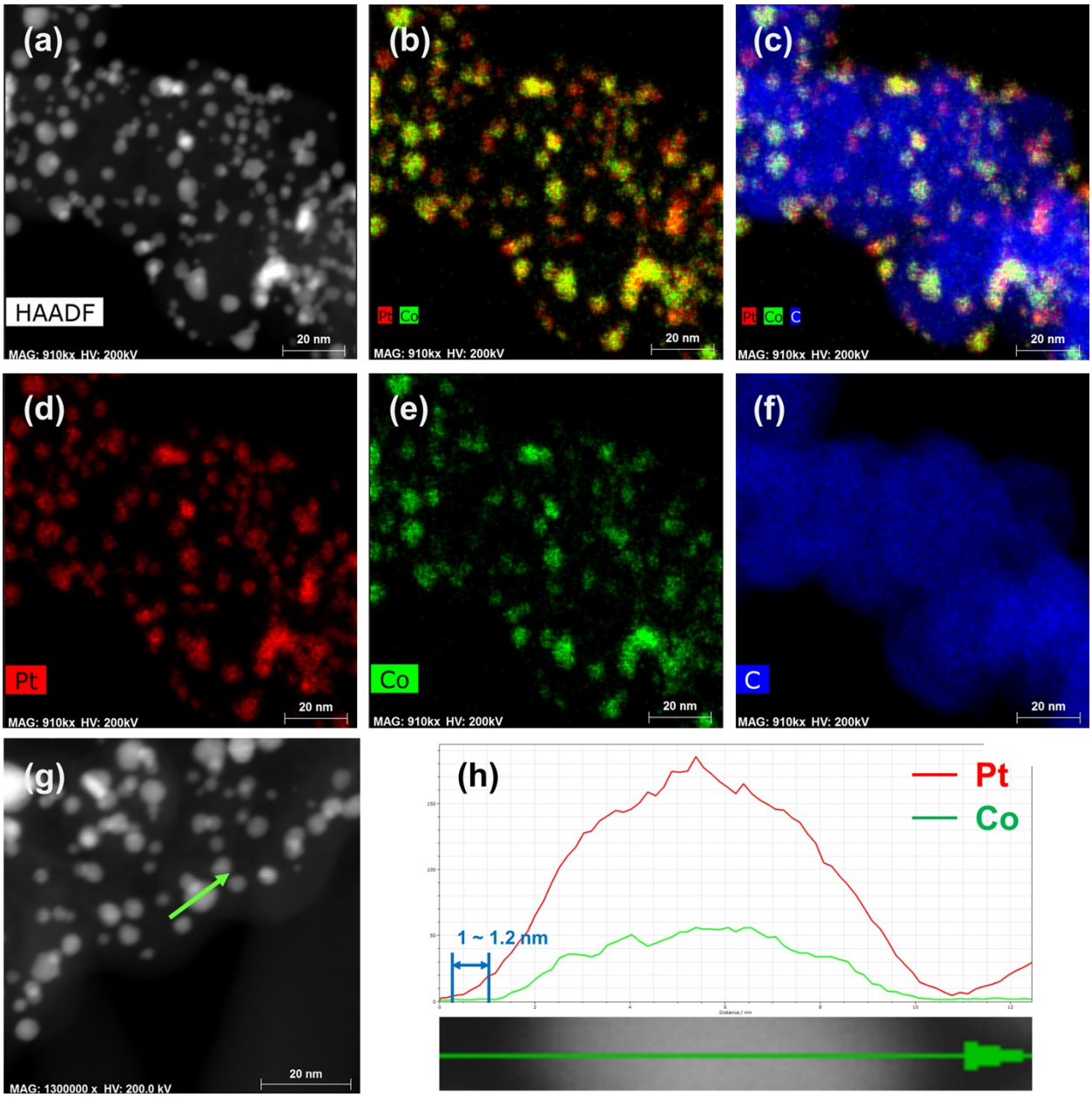

Figure S4. (a) HAADF-STEM image of PtCo/NGC which heat-treated the Pt/Co@CN/GC catalyst for 30 min. EDS elemental mapping images of PtCo/NGC (30 min): (b, c) overlap, (d) Pt, (e) Co, and (f) carbon. (g, h) EDS cross-sectional compositional line profile of PtCo/NGC (30 min).

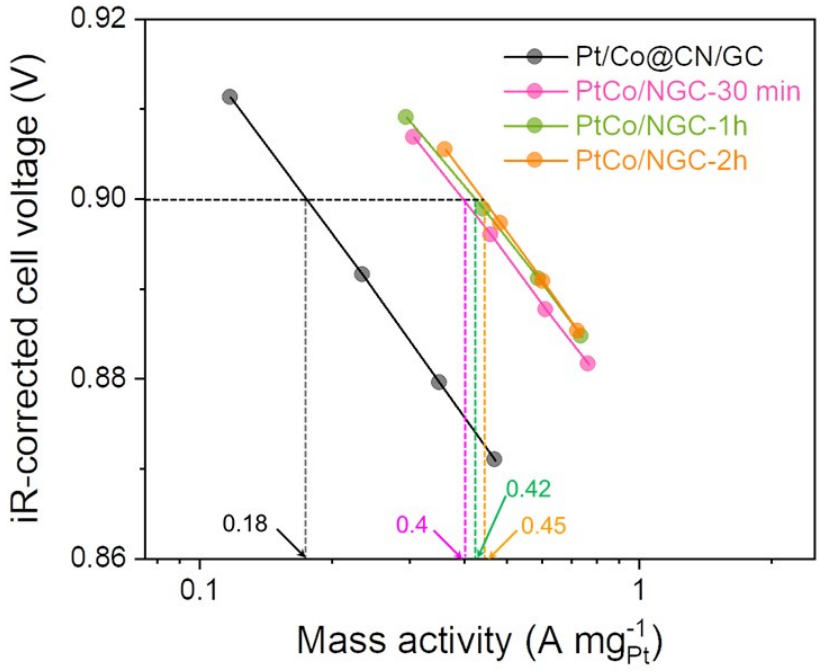

Figure S5. Mass activity of Pt/Co@CN/GC and PtCo/NGC with different heat-treatment duration time (30 min, 1 h and 2 h) at 800 ℃. Commercial Pt/C (TEC10E50E, Tanaka Kikinzoku Kogyo K.K.) was used as a catalyst for the anode.

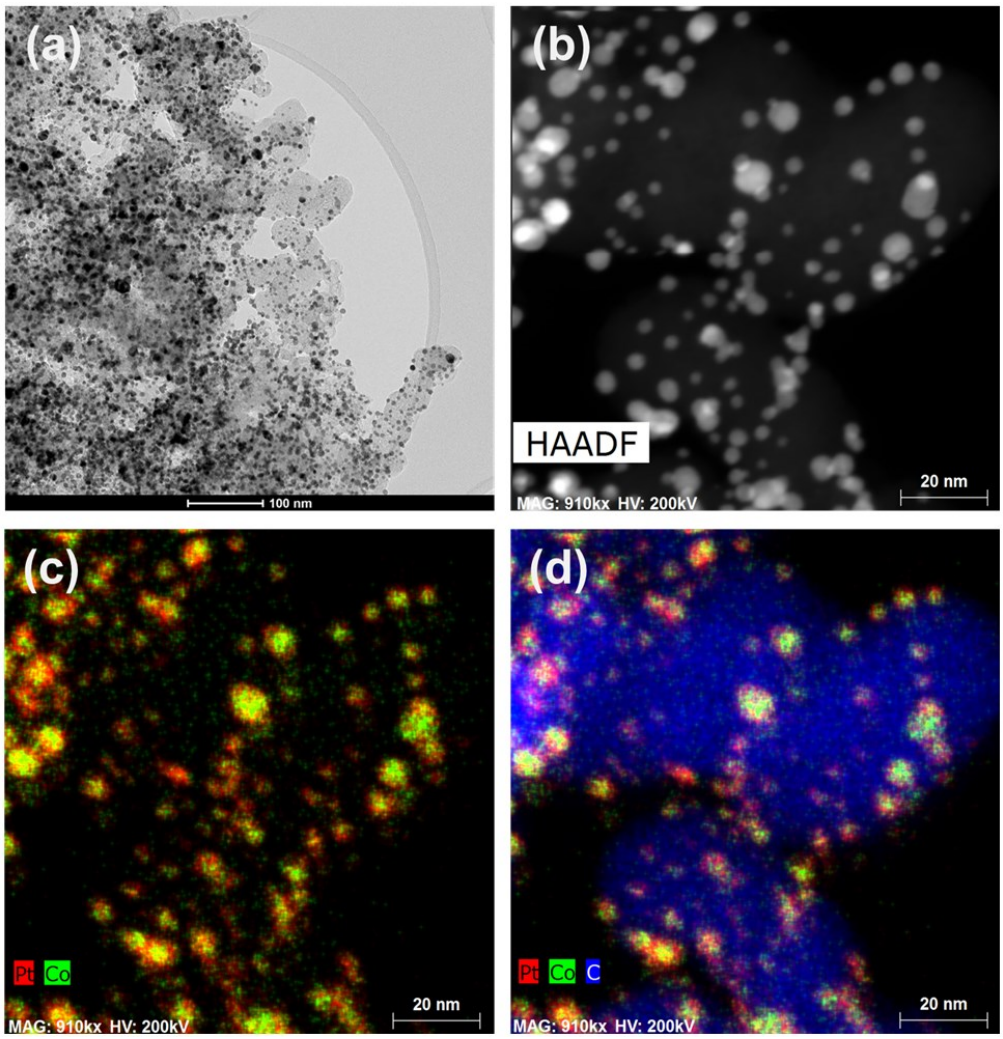

Figure S6. (a) HR-TEM and (b) HAADF-STEM images of PtCo/NGC after AST measurement. (c, d) Elemental mapping images of PtCo/NGC: Pt (red), Co (green), and Carbon (blue).

Table S4. Summary of the accelerated stress test (AST) results for oxygen reduction reaction in PEMFCs

Catalysts (Pt loading at cathode)	Cell Temp. [°C]	AST conditions (cycle No. and potential range)	Initial mass activity @ 0.9 $V_{iR\text{-}free}$ [A mg^{-1}]	Activity loss [%]	Initial ECSA [m^2 g_{Pt}^{-1}]	ECSA loss [%]	Performance loss	Ref No.
PtCo/NGC (0.1 mg cm^{-2})	80	30,000 cycles (0.6 – 1.0 V)	0.45	53	74	27	34 mV at 800 mA cm^{-2}	This work
$Pt_{2.6}Co$ TONs/C (0.1 mg cm^{-2})	80	30,000 cycles (0.6 – 0.95 V)	0.294	24	99	17	-	Xia et al. (1)
PtNi@Pt/C (0.2 mg cm^{-2})	80	30,000 cycles (0.6 – 1.0 V)	-	-	-	22	ca. 100 mV at 800 mA cm^{-2}	Lee et al.* (2)
Ga−PtNi/C (0.15 mg cm^{-2})	65	30,000 cycles (0.6 – 1.0 V)	-	-	-	-	33% loss (current density) at 0.6 V	Cho et al. (3)
Pt/IrO_2-TiO_2 (0.45 mg cm^{-2})	80	10,000 cycles (0.6 – 1.0 V)	0.088	19	43	60	100 mV at 800 mA cm^{-2}	Kotz et al. (4)
Pd/C@Pt_{skin} (0.033 mg cm^{-2})	65	30,000 cycles (0.6 – 1.0 V)	0.3	-	92.3	-	-	Hou et al. (5)
Dealloyed $PtNi_3$/C (0.1 mg cm^{-2})	80	30,000 cycles (0.6 – 1.0 V)	0.5	0	37	29	-	Mukerjee et al. (6)
CNF/TiO_2-Pt (0.4 mg cm^{-2})	75	-	0.282	-	44.97	-	-	Shul et al. (7)
GO coated Pt/C (0.2 mg cm^{-2})		30,000 cycles (0.6 – 1.0 V)	-	-	48.8	33	-	Rafailovich et al. (8)
Pt on NbO_x/C (0.1 mg cm^{-2})	80	30,000 cycles (0.6 – 0.95 V)	0.328	36	29	51	-	Xu et al. (9)
PtNi/C (0.1 mg cm^{-2})	80	30,000 cycles (0.6 – 1.0 V)	-	58	42.4	59	ca.50 m $V_{iR\text{-}free}$ at 800 mA cm^{-2}	Mustain et al.* (10)
PtCuCO/C (0.2 mg cm^{-2})	80	30,000 cycles (0.5 – 1.0 V)	0.42	40.5	-	51	-	Strasser et al. (*11*)

* Performance loss represented here is estimated from V-i polarization curves.

References

1. M. Shen, M. Xie, J. Slack, K. Waldrop, Z. Chen, Z. Lyu, S. Cao, M. Zhao, M. Zhao, M. Chi, P. N. Pintauro, R. Cao, Y. Xia, Pt-Co truncated octahedral nanocrystals: a class of highly active and durable catalysts toward oxygen reduction. *Nanoscale* **12**, 11718-11727 (2020).
2. J. Choi, J. Jang, C. Roh, S. Yang, J. Kim, J. Lim, S. J. Yoo, H. Lee, Gram-scale synthesis of highly active and durable octahedral PtNi nanoparticle catalysts for proton exchange membrane fuel cell. *Applied Catalysis B: Environmental* **225**, 535-537 (2018).
3. J. Lim, H. Shin, M. Kim, H. Lee, K. Lee, Y. Kwon, D. Song, S. Oh, H. Kim, E. Cho, Ga–doped Pt–Ni octahedral nanoparticles as a highly active and durable electrocatalyst for oxygen reduction reaction. *Nano Letters* **18**, 2450-2458 (2018).
4. A. Pătru, A. Rabis, S. E. Temmel, R. Kotz, T. J. Schmidt, Pt/IrO2–TiO2 cathode catalyst for low temperature polymer electrolyte fuel cell–Application in MEAs, performance and stability issues. *Catalysis Today* **262**, 161-169 (2016).
5. S. Hong, M Hou, H. Zhang, Y. Jiang, Z. Shao, B. Yi, A high-performance PEM fuel cell with ultralow platinum electrode via electrospinning and underpotential deposition. *Electrochimica Acta* **245**, 403-409 (2017).
6. Q. Jia, J. Li, K. Caldwell, D. E. Ramaker, J. M. Ziegelbauer, R. S. Kukreja, A. Kongkanand, S. Mukerjee, Circumventing metal dissolution induced degradation of Pt-alloy catalysts in proton exchange membrane fuel cells: revealing the asymmetric volcano nature of redox catalysis. *ACS Catalysis* **6**, 928-938 (2016).
7. Y. Jeon, Y. Ji, Y. I. Cho, C. Lee, D. Park, Y. Shul, Oxide–carbon nanofibrous composite support for a highly active and stable polymer electrolyte membrane fuel-cell catalyst. *ACS nano* **12**, 6819-6829 (2018).
8. L. Wang, S. Bliznakov, R. Isseroff, Y. Zhou, X. Zuo, A. Raut, W. Wang, M. Cuiffo, T. Kim, M. H. Rafailovich, Enhancing proton exchange membrane fuel cell performance via graphene oxide surface synergy. *Applied Energy* **261**, 114277 (2020).
9. C. Xu, J.Yang, E. Liu, Q. Jia, G. M. Veith, G. Nair, S. D. Pietro, K. Sun, J. Chen, P. Pietrasz, Z. Lu, M. Jagner, K. K. Gath, S. Mukerjee, J. R. Waldecker, Physical vapor deposition process for engineering Pt based oxygen reduction reaction catalysts on NbOx templated carbon support. *Journal of Power Sources* **451**, 227709 (2020).
10. X. Peng, S. Zhao, T. J. Omasta, J. M. Roller, W. E. Mustain, Activity and durability of Pt-Ni nanocage electocatalysts in proton exchange membrane fuel cells. *Applied Catalysis B: Environmental* **203**, 927-935 (2017).
11. K. C. Neyerlin, R. Srivastava, C. Yu, P. Strasser, Electrochemical activity and stability of dealloyed Pt–Cu and Pt–Cu–Co electrocatalysts for the oxygen reduction reaction (ORR). *Journal of Power Sources* **186**, 261-267 (2009).